Epidural Contrast Staining in High Cervical Micro-Arteriovenous Fistulae

Marlise P. dos Santos, Charles Haw, Fabio Settecase, Jason Chew

Keywords: Subarachnoid hemorrhage, Intracranial, Arteriovenous fistula, Dural, Vertebral artery, Computed tomography angiography, Cerebral angiography, Epidural space, Spinal

doi:10.1017/cjn.2021.51 Can J Neurol Sci. 2022; 49: 129–132

High cervical dural arteriovenous fistulae (hc-dAVF) are extremely rare causes of aiSAH.[1,2] Often neglected at DSA, approximately one-third of these cases require a repeat DSA.[3] The hc-dAVF presenting with aiSAH most commonly drain rostrally and extradurally, with or without an arterialized venous varix or outpouching, which will facilitate visual detection on DSA even if it does not reach the intracranial cavity.[3,4] The second most common pattern of venous drainage associated with aiSAH is via a radicular vein draining into the intramedullary coronal venous plexus, which may hinder diagnosis by DSA.[2,3,5] Rarely, hc-dAVF drain exclusively into the spinal or intracranial posterior fossa epidural space, imposing a considerable challenge for DSA detection.[2,5,6] We present two rare cases of micro hc-dAVF associated with aiSAH, where the detection of arterial epidural contrast staining increased diagnostic accuracy.

Case 1

A hypertensive and dyslipidemic female in her early 70s presented on day 0 of an acute severe headache associated with rapidly progressive loss of consciousness secondary to a World Federation of Neurological Surgeons grade 4 aiSAH. The CT scan showed a Fisher grade 3 diffuse aiSAH, centered predominantly in the left pontomedullary and peri-mesencephalic cisterns (Figure 1A), associated with the intraventricular hemorrhagic spread and moderate communicating hydrocephalus (Figure 1B). The CTA acquisition was suboptimal and within normal limits. The patient underwent an emergent extraventricular drainage procedure followed by DSA under general anesthesia.

On a Philips AlluraClarity FD20/20 Biplane System (Release 8.1.17, Philips Medical System, Best, the Netherlands), the 2D-DSA of bilateral internal/external carotid and ascending pharyngeal arteries and thyrocervical and costocervical trunks were within normal limits. The left VA 2D-DSA was obtained using full-strength iodinated contrast medium (Omnipaque 300; GE Healthcare Ireland, Cork, Ireland) injected at a rate of 4 ml/s with a total volume of 8 ml, which revealed a tiny arterialized intradural radicular vein along the trajectory of the left C2 nerve root (Figure 1C and D). Under controlled apnea, a left VA rotational angiogram was acquired using a 4-second standard propeller rotation of the motorized frontal C-arm at 75 kW with full-field detector format (42 cm) and full-strength contrast medium at the rate of 3 ml/s for a total volume of 18-ml with a 2.5-second start delay for maximum contrast filling of the basilar artery trunk. The acquisition dataset was post-processed for orthogonal reconstruction in the Philips 3D-RA 6.5 Interventional Workspot workstation (Philips Medical Systems Nederland B.V., Best, the Netherlands) using the XperCT software with automatic resolution (384^3 pixels) and manual windowing. This showed an abnormal contrast staining or opacification of the posterolateral epidural space at the level of C1 and C2 vertebrae (Figure 1E–G), which helps to confirm a micro hc-dAVF. The patient underwent emergency neurosurgery, where a tortuous intradural vein tangled in one of the left-sided rootlets of C2 was identified. This vein filled early on the arterial phase of the intraoperative indocyanine green video angiography and was properly coagulated. A postoperative left vertebral 2D-DSA (Figure 2A–B) and its corresponding 3D-DSA reformats (Figure 2C–E) confirmed the cure of the micro hc-dAVF. At 160 d, her mRS was 1, due to persistent occasional vertigo.

Case 2

A previously healthy and normotensive female in her mid-60s had two syncopal episodes while skiing. Her Glasgow Coma Scale was 7. She was intubated at the scene. Upon arrival on day 0, her CT head (Figure 3A–B) revealed a Fisher grade 3, predominantly left posterior fossa, aiSAH. Initial CTA (128-slice

From the Division of Neuroradiology, Vancouver General Hospital, Department of Radiology, University of British Columbia, Vancouver, BC, Canada (MPdS, FS, JC); Neuroradiology and Interventional Neuroradiology Sections, The Ottawa Hospital, Department of Medical Imaging, University of Ottawa, Ottawa, ON, Canada (MPdS); Ottawa Hospital Research Institute, Brain and Mind Research Institute, Ottawa, ON, Canada (MPdS); Division of Neurosurgery, Department of Surgery, University of British Columbia, Vancouver, BC, Canada (CH); Department of Medical Imaging, Vancouver General Hospital, Gordon and Leslie Diamond Health Care Centre, Vancouver, BC, Canada (CH); and Vancouver Coastal Health Research Institute, Vancouver, BC, Canada (CH, FS, JC)

Received May 26, 2020. Final Revisions Submitted February 6, 2021. Date of Acceptance March 14, 2021.

Correspondence to: Marlise P. dos Santos, University of Ottawa, Diagnostic and Interventional Neuroradiologist, The Ottawa Hospital, 01-1-10A, 1053 Carling Avenue, Ottawa, ON, Canada K1Y 4E9. Email: msantos@toh.ca

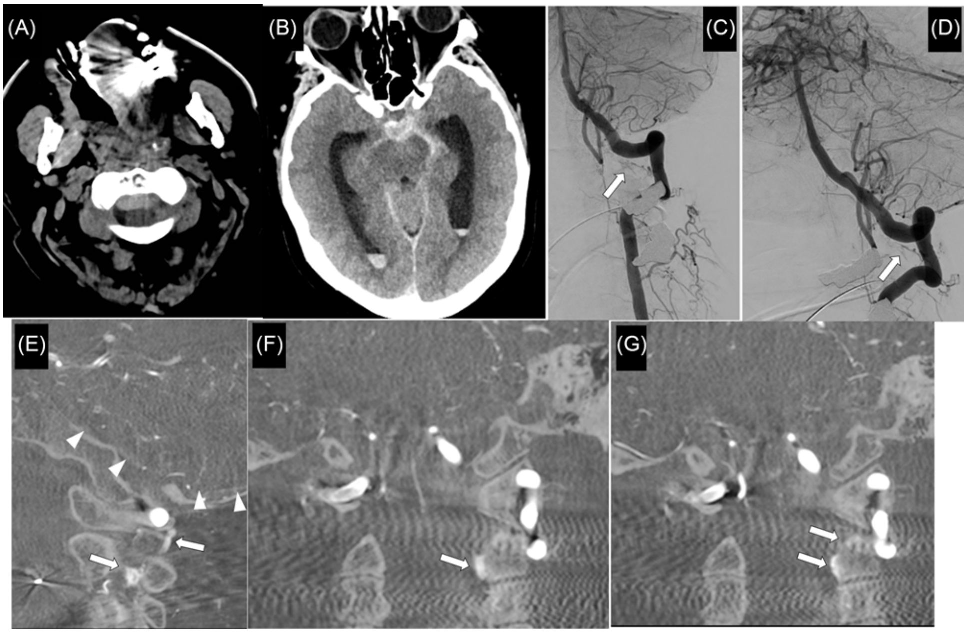

Figure 1: *Case 1. Pre-operative imaging. Non-contrast CT head: upper cervical SAH (A) with ponto-medullary, peri-mesencephalic and suprasellar cistern extension (B) with moderate hydrocephalus. Left vertebral 2D-DSA on anteroposterior (C) and left anterior oblique (D) projections depicting a hc-dAVF fed by a left C2 radicular artery shunting into a tiny intradural radicular vein (white arrows). Multiplanar reconstruction of the left vertebral 3D-DSA on the early arterial phase (2.5-second contrast injection delay): (E) sagittal plane white arrows indicating iodinated contrast staining into the epidural space/veins at C2 vertebral level, confirmed on the axial (not shown) and on the white arrows on the coronal views (F) and (G). Note the relatively lower density of the subarachnoid hemorrhage (arrow heads) as compared with the density of the contrast (E).*

SOMATOM Definition Flash, Siemens Healthineers Global, Erlangen, Germany) showed dilated intramedullary veins at the C1–C2 level concerning for a hc-dAVF. Bilateral vertebral 2D-DSA confirmed a micro hc-dAVF fed symmetrically by C2 radicular arteries associated with early intramedullary and epidural venous drainage without vascular ectasia (Figure 3C and D; *right VA injection is not shown*). A 3D-DSA was not performed. A retrospective evaluation of the initial CTA revealed an asymmetrical arterial contrast enhancement of the anterolateral epidural space from the foramen magnum to C2 with density mirroring normal neck arteries (Figure 3E and F). The patient underwent a partial trans-arterial embolization of the right VA feeder to the hc-dAVF (complicated by a right VA iatrogenic dissection) followed by a successful surgical disconnection of bilateral arterialized intradural veins. On day 33, a CTA (Figure 3G) demonstrated the absence of asymmetrical epidural contrast staining. A post-therapeutic DSA was avoided due to the complicated course of her trans-arterial embolization. At 120 d, her mRS was 0.

To our knowledge, this is the first report of epidural contrast staining detection using either high-resolution 3D-DSA reconstruction reformats and/or CTA for the confirmation of an hc-dAVF. Our techniques are readily adaptable to any DSA equipment with 3D/rotational capability and to any multi-slice CT scanner and could facilitate detection of a cause for aiSAH in patients with negative DSA or CTA. Because the total dose of contrast used in 3D-DSA is at least three times higher than in 2D-DSA, the spatial resolution of 3D-DSA is higher than 2D-DSA. The high-resolution multiplanar reformats with manual windowing allow for the unique identification of subtle areas of early enhancement of arterialized venous structures. The orthogonal reformation of properly centered and well-timed 3D-DSA displays the abnormal early contrast opacification of a micro hc-dAVF. The time delay in seconds for the 3D-DSA pump contrast injection is set based on how long the iodinated contrast takes to fill the target vessel on 2D-DSA. When this method fails to demonstrate an hc-dAVF, a 3D-DSA of specific or suspicious arteries using similar, but properly adjusted contrast dosage, injection rate, and timing should be considered while being mindful of the radiation exposure and procedure time. A CTA with "pure" arterial phase obtained using a multi-slice CT scanner may depict arterial contrast staining into structures that would normally only enhance in the venous phase. A helpful rule of thumb is to compare the density of the suspicious contrast staining against the density of a large normal vein of the neck in the same CTA slice (Figure 3E–G). Abnormal arterial contrast staining will mirror that of regional arteries rather than veins. With the goal of improving diagnostic accuracy in nonaneurysmal aiSAH, future studies can look at the accuracy of 4D/time-resolved CTA for detection of hc-dAVF.

https://doi.org/10.1017/cjn.2021.51 Published online by Cambridge University Press

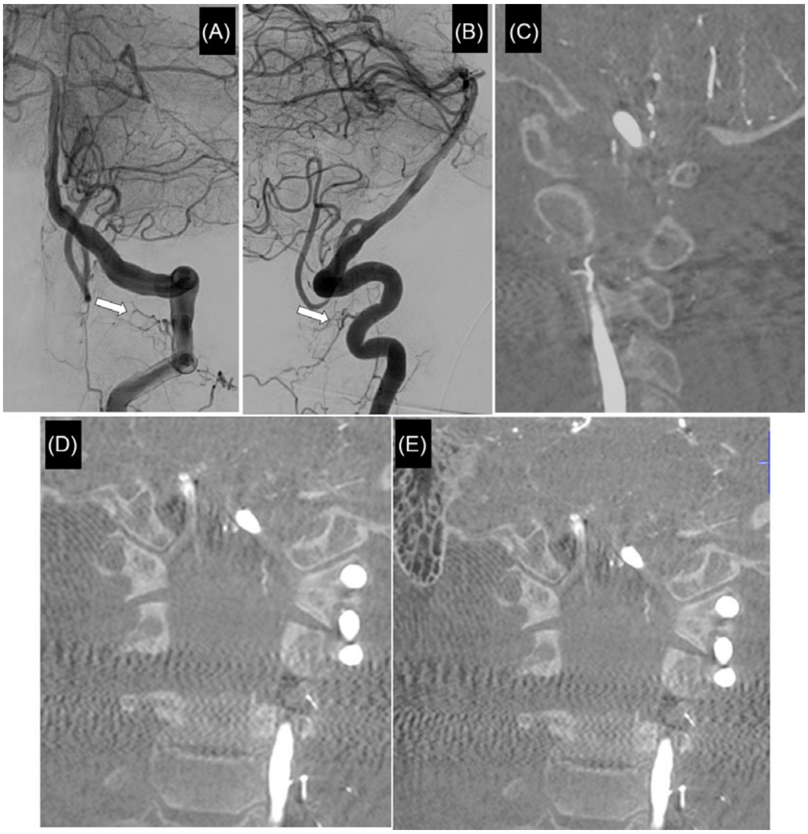

Figure 2: *Case 1. Post-operative imaging. Left vertebral 2D-DSA on anteroposterior (AP) and straight lateral (B) projections showing the C2 radicular artery without residual arteriovenous shunting or arterialized vein (arrows). Multiplanar reconstruction of left vertebral 3D-DSA on early arterial phase (2.5-second contrast injection delay): absence of iodinated contrast staining of the epidural space/veins at the atlantoaxial and upper cervical levels, confirmed on the axial (not shown), sagittal (C) and coronal views (D-E).*

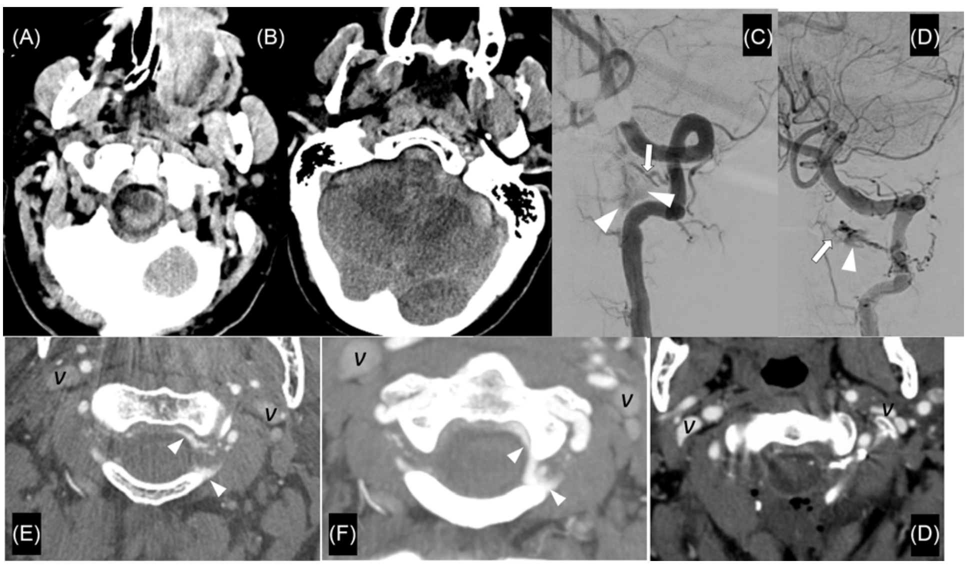

Figure 3: *Case 2. Non-contrast CT head: diffuse aiSAH extending below the foramen magnum (A) and into the left pontomedullary cistern (B). Left vertebral 2D-DSA on straight (C) and Townes anteroposterior (D) projections depicting the most probable fistulous point (white arrows) between a prominent left C2 radicular artery and a tiny arterialized intradural radicular vein with contrast enhancement of the epidural drainage of the fistula (arrow heads). There was an identical hc-dAVF from the right VA 2D-DSA (not shown). Initial CTA: asymmetrical iodinated contrast staining in the left C1-C2 anterolateral epidural space noted, in retrospect, on the axial 0.6-mm thick source images (E) and on the 4-mm axial MIPs (F) of the initial CTA (arrow heads). Repeat CTA after endovascular and surgical hc-dAVF disconnections (G): resolution of the asymmetrical contrast staining. Note the relative low density of the iodinated contrast in the internal jugular veins (v).*

https://doi.org/10.1017/cjn.2021.51 Published online by Cambridge University Press

Acknowledgements

The authors thank Betty Anne Schwarz, PhD, for the editing support.

Statement of Authorship

MPdS: Conceptualization; Supervision; Methodology; Roles/ Writing – original draft; Writing – review and editing; CH: Methodology; Writing –review and editing; FS: Methodology; Roles/Writing – original draft; Writing – review and editing; JC: Conceptualization; Supervision; Methodology; Roles/Writing – original draft; Writing – review and editing.

Conflict of Interest

The authors have no conflicts of interest to disclose.

References

1. Mohan M, Islim AI, Rasul FT, et al. Subarachnoid haemorrhage with negative initial neurovascular imaging: a systematic review and meta-analysis. Acta Neurochir (Wien). 2019;161:2013–26. doi: 10.1007/s00701-019-04025-w
2. Willinsky R, Terbrugge K, Lasjaunias P, Montanera W. The variable presentations of craniocervical and cervical dural arteriovenous malformations. Surg Neurol. 1990;34:118–23. doi: 10.1016/0090-3019(90)90107-Z
3. Aviv RI, Shad A, Tomlinson G, et al. Cervical dural arteriovenous fistulae manifesting as subarachnoid hemorrhage: report of two cases and literature review. Am J Neuroradiol. 2004;25: 854–858.
4. Lucas J, Jones J, Farin A, Kim P, Giannotta S. Cervical Spine Dural Arteriovenous Fistula With Coexisting Spinal Radiculopial Artery Aneurysm Presenting as Subarachnoid Hemorrhage: Case Report. Neurosurgery. 2012;70:E259–63. doi: 10.1227/NEU.0b013e31822ac0fb
5. Ogawa A, Furuya K, Ueno T, Naito Y, Nakagomi T. Characteristics and treatment of dural and perimedullary arteriovenous fistula at the craniocervical junction presenting with subarachnoid hemorrhage. No Shinkei Geka. 2012;40:121–8.
6. Ikeda H, Fujimoto Y, Koyama T, Fujimoto Y. A rare case of high cervical spinal cord dural arteriovenous fistula presenting with intracranial subarachnoid hemorrhage. No Shinkei Geka. 1994;22:1045–8.